Distribution of Suspended Sediment in Large Waves

By Jørgen Fredsøe,[1] Ole H. Andersen,[2] and Steen Silberg[3]

Abstract: The distribution of suspended sediment in the combined wave-current motion is theoretically predicted in the case of a plane bed. This will be the case if the wave-induced motion close to the bed is sufficiently strong. The theory is able to predict the average value of the concentration as well as the instantaneous values at a given distance from the bed. The theory is compared with laboratory and field measurements.

Introduction

The vertical distribution of suspended sediment in combined wave-current motion is of interest when evaluating the sediment transport in the sea.

The ordinary way to describe the vertical distribution of suspended sediment is to apply the diffusion equation

$$\frac{dc}{dt} = w\frac{\partial c}{\partial y} + \frac{\partial}{\partial y}\left(\epsilon_s \frac{\partial c}{\partial y}\right) \quad \ldots\ldots (1)$$

where c = concentration by volume; t = time; w = fall velocity of suspended sediment; y = the vertical coordinate; and ϵ_s = the turbulent exchange factor for suspended sediment. In Eq. 1, the horizontal diffusion terms are neglected, because the vertical gradient of suspended sediment is much larger than the horizontal one.

ϵ_s is normally taken to be equal to (or proportional to) the eddy viscosity ϵ of the flow. In the present paper, we take $\epsilon_s = \epsilon$.

In ordinary, steady, open-channel flow, the vertical distribution of c has been known for decades. It is obtained from Eq. 1 by applying the well-known parabolic distribution for the eddy viscosity

$$\epsilon = \kappa U_f y\left(1 - \frac{y}{D}\right) \quad \ldots\ldots (2)$$

where $\kappa \simeq 0.4$ = the von Kármán constant; U_f = the shear velocity; and D = the water depth. Inserting Eq. 2 into Eq. 1 and considering the steady solution ($\partial c/\partial t = 0$), we obtain the following solution:

$$\frac{c}{c_a} = \left(\frac{D-y}{y}\frac{a}{D-a}\right)^{w/\kappa U_f} \quad \ldots\ldots (3)$$

(17), where c_a = the concentration at a certain distance, a, above the bed.

[1]Assoc. Prof., Inst. Hydrodynamics and Hydr. Engrg., ISVA, Tech. Univ. of Denmark, Lyngby, Denmark.

[2]Master of Sci. in Civ. Engrg., Tech. Univ. of Denmark, Lyngby, Denmark.

[3]Master of Sci. in Civ. Engrg., Tech. Univ. of Denmark, Lyngby, Denmark.

Note.—Discussion open until April 1, 1986. To extend the closing date one month, a written request must be filed with the ASCE Manager of Journals. The manuscript for this paper was submitted for review and possible publication on September 14, 1983. This paper is part of the ***Journal of Waterway, Port, Coastal and Ocean Engineering***, Vol. 111, No. 6, November, 1985. ©ASCE, ISSN 0733-950X/85/0006-1041/$01.00. Paper No. 20168.

Now, returning to oscillatory flow, we are faced with the question how much the problem can be simplified when solving the similar problem of vertical distribution. Two different approaches can be suggested.

1. The most simple one will be the adoption of an expression of the eddy viscosity like Eq. 2, averaged over one wave period in oscillatory flow. Such an expression was suggested by Lundgren (11), who constructed the expression

$$\epsilon_w = \frac{\kappa U_{f,\max} y}{\left[1 + 1.34 \sqrt{\frac{1}{2} f_w} \frac{y}{\delta_1} \exp\left(\frac{y}{\delta_1}\right)\right]} \quad \ldots\ldots (4)$$

where $U_{f,\max}$ = maximum shear velocity during one wave period; f_w = wave friction factor; and δ_1 = mean boundary layer thickness. Eq. 4 is empirically based on the measurements in Refs. 9 and 19. Since Eq. 4 is the mean averaged value over one wave period, Eq. 1 can easily be solved by putting $\partial c/\partial t = 0$, to give

$$C = K y^{-w/\kappa U_f} \exp\left[-\frac{w}{\kappa U_f} 1.34 \sqrt{\frac{1}{2} f_w} \exp\left(\frac{y}{\delta_1}\right)\right] \quad \ldots\ldots (5)$$

where C = the mean concentration (averaged over one wave period); and K = a constant to be determined from the boundary condition at the bed.

2. A more correct and detailed approach to the problem will be to take the starting point in Eq. 1, calculating the time and space variations in c during one wave period. Hereby, it will be possible to take into account the time variation in the eddy viscosity and to introduce the boundary condition at the bed in a more rigorous manner.

Procedure 1 cannot describe the mean concentration correctly, as illustrated by the following example.

Let us consider a periodic unsteady motion, which during the first half-period, $T/2$, has a constant flow velocity, V_1, and during the second has the velocity zero. If we now assume T to be so large that the time-scale for the settling of suspended sediment is much smaller than T the correct distribution will be

$$C = \frac{1}{2} c_{a1} \left(\frac{D - y}{y} \frac{a}{D - a}\right)^{w/\kappa U_{f1}} \quad \ldots\ldots (6)$$

where U_{f1} = the friction velocity according to the mean flow velocity V_1; and c_{a1} = the bed concentration determined from the conditions at flow velocity V_1. If, instead, we solve the diffusion equation based on the mean eddy viscosity during the total period of motion, this eddy viscosity will be only half the eddy viscosity for flow velocity V_1. So, Eq. 1 gives

$$C = c_{a2} \left(\frac{D - y}{y} \frac{a}{D - a}\right)^{2w/\kappa U_{f1}} \quad \ldots\ldots (7)$$

where c_{a2} = a nominal concentration different from c_{a1}. It can easily be seen that even by an appropriate choice of c_{a2}, Eqs. 6 and 7 cannot be identical.

Scope of Present Work

As far as the writers know, Ref. 2 is the only attempt hitherto made at following procedure 2 described in the previous section. In Ref. 2, the time and space variations in eddy viscosity were found by calculating the oscillatory flow and introducing the mixing length hypothesis. The present flow description, which is referred to in detail in Ref. 6, is based on the idea that the unsteady flow can be regarded as a growing boundary layer, where a new boundary layer develops every time the flow reverses. This gives a simple mathematical tool for a description of the process by which the sediment is brought into suspension during the large near-bed flow velocities and carried away from the bed at the end of each half of a wave cycle because of the expansion of the boundary layer. When the flow reverses the new boundary layer is at first very thin and the sediment away from the bed settles with the fall velocity until it is entrained into the boundary layer.

As pointed out in Ref. 6, the present flow model is very simple to handle, requiring only the solution of an ordinary first-order differential equation, while Ref. 2 requires the solution of a second-order nonlinear partial differential equation. This may be important if the sediment model is implemented in a larger mathematical flow model to describe the general offshore sediment movement in a large area.

Another advantage of the present flow description is that it can be extended with only minor modifications to describe the boundary layer and, thus, the concentration distribution in a more complex wave-current motion. In the present paper, we restrict ourselves to sinusoidal wave motion, but the flow model (6) can describe the boundary layer for nonlinear waves too. Thus, the present model may be a tool for calculating on-shore/off-shore sediment movements and related problems. Finally, in the present model the current direction may have an arbitrary angle with the direction of wave movement. Refs. 2 and 3 only cover the two-dimensional case.

The sediment description differs from Bakker's (2) mainly by introducing another model for the bed concentration described in Ref. 5. Ref. 2 applies the approach of Kalkanis (10), which is based on Einstein's geometrical method (4). The model of Ref. 5 is based on dynamic considerations, whereby it becomes more obvious that the instantaneous bed concentration is determined by the instantaneous bed shear stress.

The bed is assumed to be planar, which is in accordance with the fact that ripples disappear at values of the dimensionless bed shear stress (the Shields parameter, θ; see Eq. 13) larger than 0.8–1.0 (see Ref. 13).

Because of the high values of the bed shear stress, the calculations carried out in the following are all taken only for a hydraulic rough bed.

Theory for Suspended Sediment in Pure Wave-Motion

Flow Description.—The flow description is based on a rather simple

flow model recently developed by Fredsøe (6).

The ideas in Ref. 6 are briefly outlined below for the case of no resulting current. We assume the velocity profile, u, in the wave boundary layer to be logarithmic and given by

$$\frac{u}{u_f} = \frac{1}{\kappa} \ln \left(\frac{y}{\frac{k}{30}} \right) \quad \ldots\ldots (8)$$

where u_f = the shear velocity; y = the distance from the bed; κ = von Kármán's constant (~0.40); and k = the bed roughness. The bed roughness of a plane bed covered by sand with a mean diameter d is about $2.5d$ due to the irregular position of the sand grains on the bed (see Ref. 5). Outside the boundary layer, the velocity is given by a periodic motion with the velocity

$$u_0 = U_{1m} \sin(\omega t) \quad \ldots\ldots (9)$$

where U_{1m} = maximum velocity occurring outside the boundary layer due to wave motion (obtained from potential theory); and ω = angular frequency (= $2\pi/T$, and T = wave period). Inserting Eq. 8 into the momentum equation

$$-u_f^2 = -\int_{k/30}^{\delta + k/30} \frac{\partial}{\partial t}(u_0 - u)\, dy \quad \ldots\ldots (10)$$

where δ = the instantaneous wave boundary thickness, the variations in time of u_f and δ are easily found when assuming a new boundary layer to develop every time the water outside the wave boundary layer starts moving (i.e., $\omega t = 0, \pi, 2\pi \ldots$). A typical variation in δ and u_f is shown in Figs. 1(*a–b*) in which a = the free stream particle amplitude.

With known friction velocity and wave boundary layer thickness we now take the vertical distribution of the eddy viscosity in the boundary layer to be parabolic as it is in steady flow

$$\epsilon = \kappa |u_f| y \left(1 - \frac{y}{\delta} \right) \quad \ldots\ldots (11)$$

If Eq. 11 is averaged over one wave period, the mean value of the eddy viscosity $\bar{\epsilon}$ has a shape similar to that developed by Lundgren (11) from Jonsson's (7) measurements. Close to the bed, $\bar{\epsilon}$ increases linearly with the distance from the bed proportionally to κU_f, with U_f = the mean value of $|u_f|$. Away from the bed $\bar{\epsilon}$ decreases to zero.

When the eddy viscosity is taken as a function of the instantaneous bed shear stress and boundary layer thickness, the memory in turbulence is not taken into account, just as it is not incorporated in the models by Bakker (2) and Bakker and Doorn (3). As long as the boundary thickness is small, the memory effects in turbulence must be rather limited, so the main error caused by neglecting the memory arises in connection with the large eddies developing at the end of each movement (where δ increases rapidly). However, these eddies have a very low velocity, so it seems reasonable to disregard this effect.

In connection with the distribution of suspended sediment, a very im-

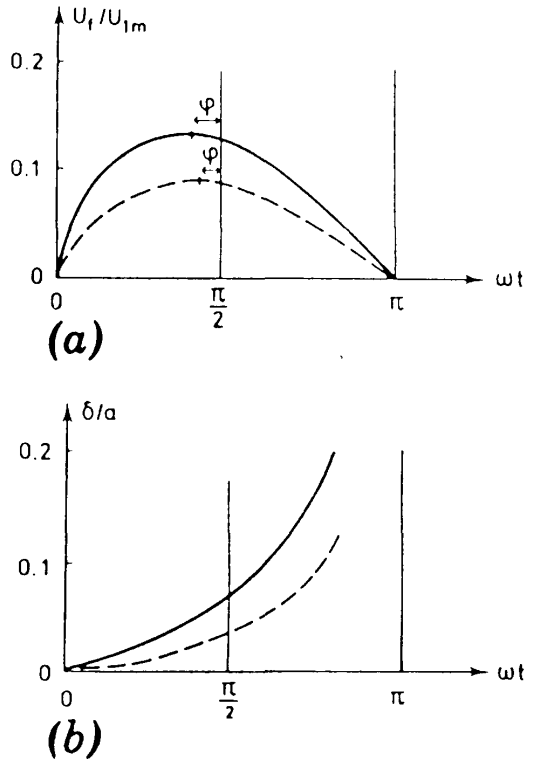

FIG. 1.—(*a*) Typical Variation in Shear Velocity; (*b*) Boundary Layer Thickness with Time during Half a Wave Cycle in Pure Wave Motion (—: a/k = 10; ---: a/k = 100)

portant memory effect arises owing to the finite fall velocity of the particles in suspension. Normally, this effect is rather large, and it justifies, as a first approximation, neglecting the memory effect in the flow itself.

Description of Sediment.—When the variations in bed shear stress and eddy viscosity are obtained, the diffusion equation for sediment, Eq. 1, can be solved numerically. To solve Eq. 1 the following boundary conditions are applied:

1. At the bed, the instantaneous concentration is assumed to be a function of the instantaneous bed shear stress. In the present work, we apply the relationship developed in Ref. 5, in which the bed concentration is calculated on the basis of Bagnold's ideas (1) of how the fluid shear stress is transferred to a bed covered by loose sediment. From Ref. 5 a functional relationship is found between the bed concentration, c_b, at a distance of the order of two grain diameters from the bed and the dimensionless bed shear stress, θ

$$c_b = c_b(\theta) \quad \ldots\ldots (12)$$

where θ is defined as

$$\theta = \frac{\tau}{\rho(s-1)gd} = \frac{u_f^2}{(s-1)gd} \quad \ldots\ldots (13)$$

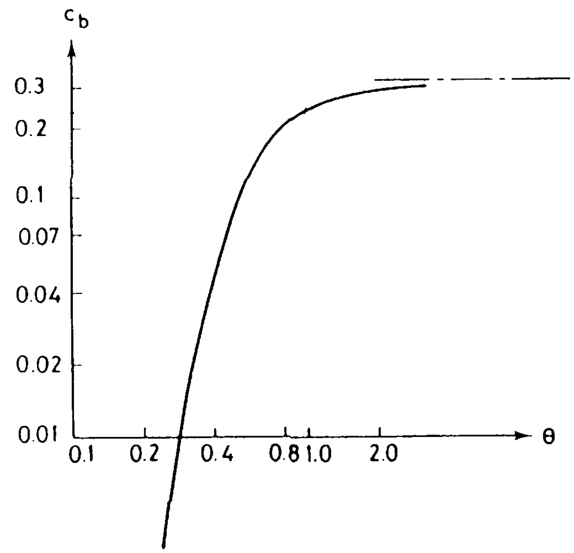

FIG. 2.—Reference Concentration at Bed from Ref. 5

where τ = bed shear stress; ρ = density of fluid; s = relative density of the grains; g = acceleration of gravity; and d = mean grain diameter. The relationship in Eq. 12 is depicted in Fig. 2; for large values of θ, c_b approaches a constant value of about 0.3. The relationship in Eq. 12 shown in Fig. 2 is a slightly changed version of the original one suggested in Ref. 5 because it has turned out that an improved description of c_b is obtained by changing the friction coefficient slightly to be equal one.

2. At the free surface, the flux of sediment is zero. Usually this becomes the same as to state that the concentration becomes zero far away from the bed.

3. The time variation in c must be periodic, so

$$c(t,y) = c(t + T, y) \quad (14)$$

Theoretical Results

In Fig. 3, the variation in c with time at different distances from the bed is shown for a specific run. Such a run can be described if the dimensionless parameters a/k, θ_{max}, and $w/U_{f,max}$ are known.

In Fig. 3, the ordinate indicates the relative concentration $c/c_{b,max}$, where $c_{b,max}$ = the bed concentration for $U_f = U_{f,max}$. $c_{b,max}$ is obtained from Fig. 2. It is seen from Fig. 3 that maximum bed shear stress (ϕ before maximum wave velocity outside the boundary layer; see Ref. 6) results in maximum concentration just above the bed (y/k = 0.8 or $y \simeq 2d$). Increasing distance from the bed causes maximum concentration to lag more and more behind maximum bed shear stress, since suspended sediment will take some time to settle after having been picked up from the bed.

Furthermore, Fig. 3 shows that the variation in c follows an asymmetric pattern; the rise in concentration occurs much faster than the fall for two reasons. First, the variation in u_f is asymmetric [see Figs. 1(a–

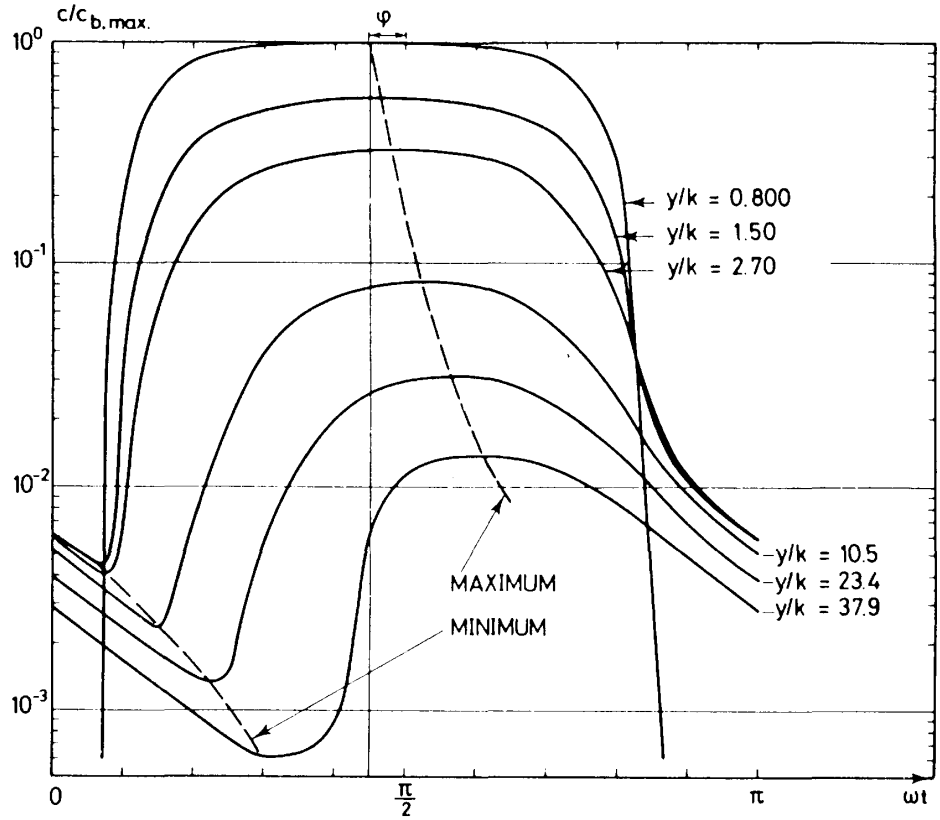

FIG. 3.—Variation in Concentration with Time at Different Levels from Bed for a/k = 3,916 (θ_{max} = 1.45; w/U_{1m} = 0.018)

b)]. However, this contribution is not very important (see Fig. 3) as the variation in the bed concentration for $y/k \simeq 0.8$ is nearly symmetric. This is because the bed concentration is negligibly sensitive to changes in bed shear stress if θ is sufficiently large (see Fig. 2). The second contribution to the asymmetric shape arises because the rise in the concentration is very rapid where the sediment is brought into suspension and pushed away from the bed during the large bed shear stresses, while the fall in concentration simply occurs because the sediment falls towards the bed at fall velocity, w, with nearly no turbulence present.

This asymmetric behavior is confirmed by some recent experiments by Staub et al. (16) carried out in an oscillating flume (see Fig. 4). In these experiments, the variation in the concentration with time was measured by means of the mechanical system described in Ref. 16. The data of the experiments were d = 0.19 mm, s = 2.65, a = 1.86 m, and T = 9.1 sec, and the measurements were made at a distance of 1.8 cm above the bed. The combination of the aforementioned data gives, in fact, the dimensionless parameter combination applied in Fig. 3 with y/k = 37.9. The fully-drawn line in Fig. 4 is the theoretical one in Fig. 3, and the agreement with the experimental data is satisfactory. In Fig. 5, some further experiments from Ref. 16 are depicted, showing the average concentration for the data described earlier at different distances from the bed.

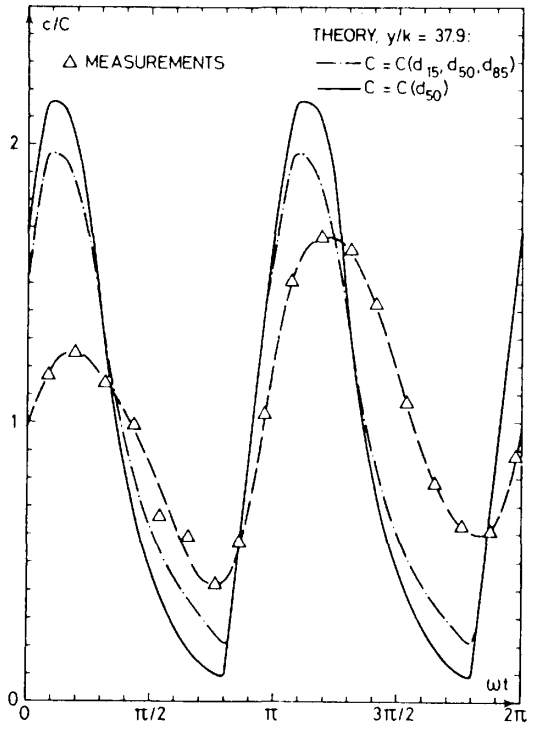

FIG. 4.—Comparison between Measured and Predicted Variation in c during One Wave Period 1.8 cm above Bed (Experimental Data: d_{50} = 0.19 mm, a = 1.86 m, T = 9.1 sec from Ref. 18; these Data Correspond to Nondimensional Data in Fig. 3; Dotted Curve: Gradation of Sediment Incorporated)

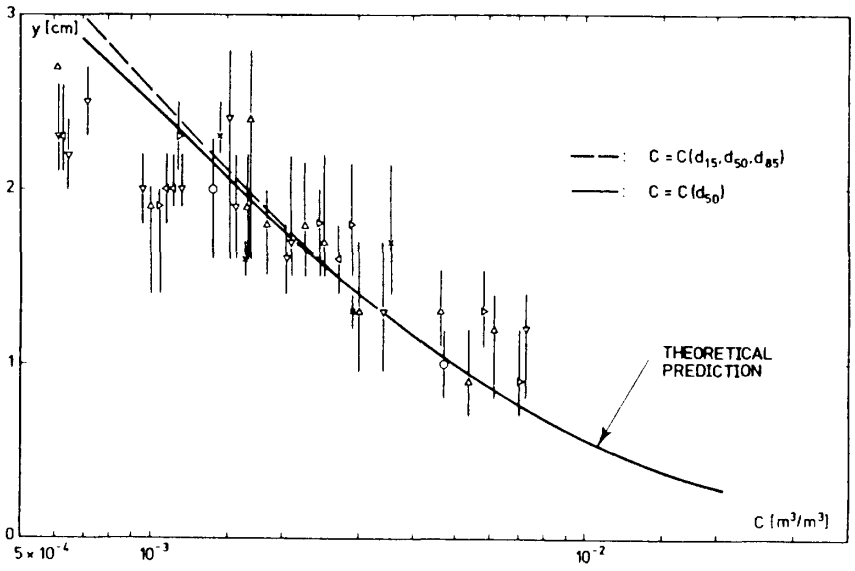

FIG. 5.—Comparison between Measured and Predicted Vertical Variation in Mean Concentration C of Suspended Sediment (Experimental Data Are Identical with those in Fig. 4 from Ref. 16; Dashed-Dotted Curve: Gradation of Sediment Incorporated)

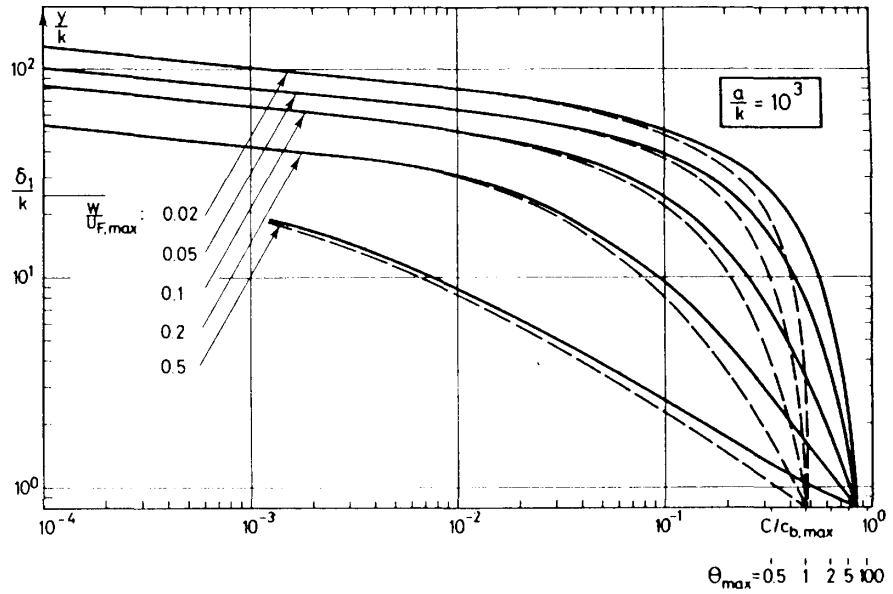

FIG. 6.—Theoretical Vertical Distribution of Average Concentration C in Pure Wave Motion for $a/k = 10^3$ (Full Drawn Line Corresponds to $\theta_{max} = 10$; Dashed Line Corresponds to $\theta_{max} = 1$)

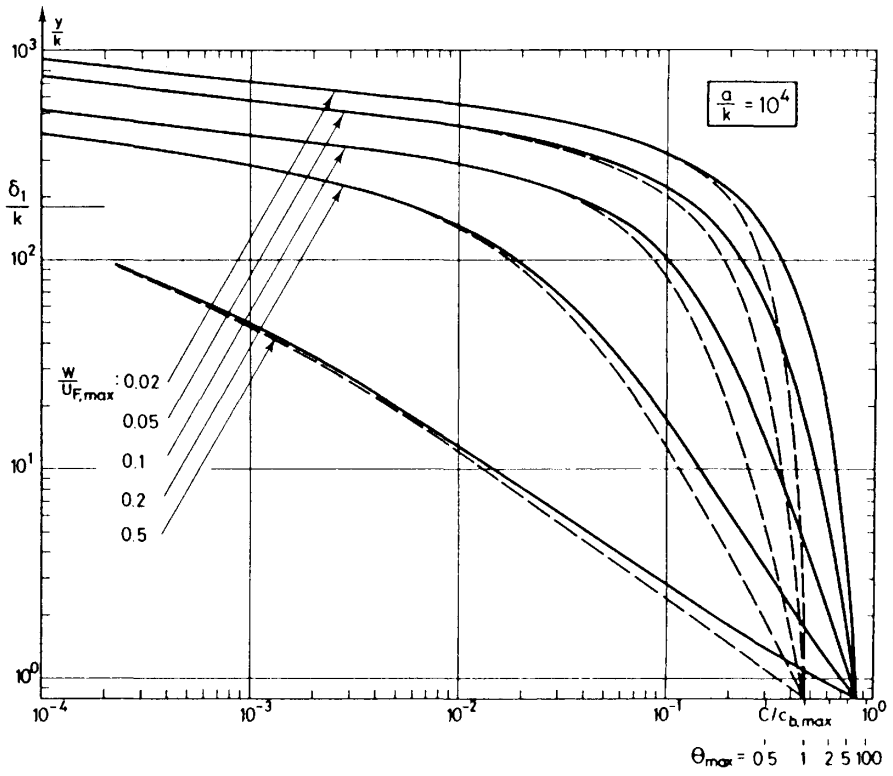

FIG. 7.—Theoretical Vertical Distribution of Average Concentration C in Pure Wave Motion for $a/k = 10^4$ (Full Drawn Line Corresponds to $\theta_{max} = 10$; Dashed Line Corresponds to $\theta_{max} = 1$)

The line surrounding each experimental point indicates the uncertainties in the measurement. These uncertainties arise from the inexact determination of the bed level, which varies slightly with time, even through only one wave period. The fully-drawn line in Fig. 5 is the theoretical prediction of the average concentration over one wave period.

Figs. 6–8 depict the average concentration C over one wave period at different combinations of the dimensionless parameters a/k, $w/U_{f,max}$, and θ_{max}. These combinations should cover most of the situations present in nature.

From the figures it will be noticed that changes in θ_{max} are important only close to the bed. The fully-drawn curves are those predicted from theory putting $\theta_{max} = 10$, while the dashed ones are based on $\theta_{max} = 1$. The starting points at the bed of the curves in the interval $1 < \theta_{max} <$

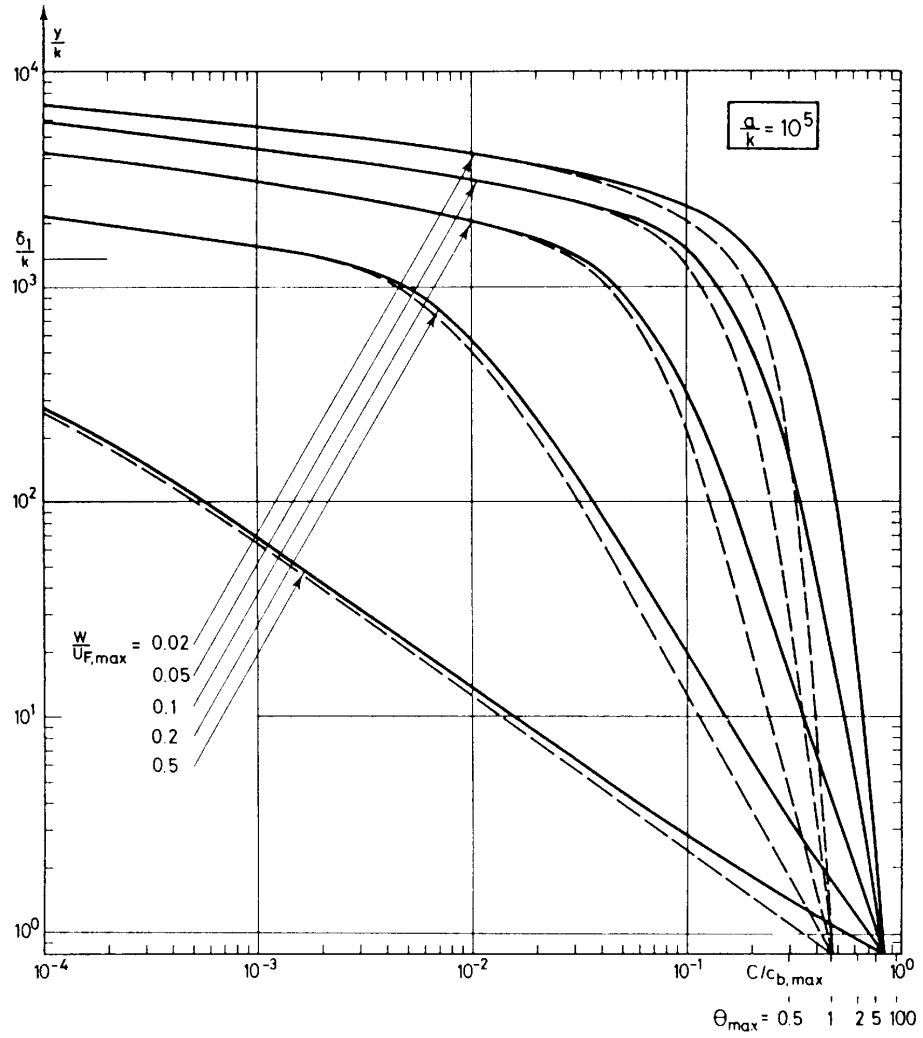

FIG. 8.—Theoretical Vertical Distribution of Average Concentration C in Pure Wave Motion for $a/k = 10^5$ (Full Drawn Line Corresponds to $\theta_{max} = 10$; Dashed Line Corresponds to $\theta_{max} = 1$)

10 are indicated along the abscissa. If θ_{max} approaches infinity, the starting point of $y/k = 0.8$ ($2d$ above the bed) should be 1.

On the ordinate the value δ_1/k indicates a kind of mean value of the turbulent boundary layer thickness, δ_1 being the boundary layer thickness at $\omega t = \pi/2$ (maximum wave-induced velocity outside boundary layer). It is seen that a significant amount of sediment may be present above this mean boundary layer thickness.

Effect of Sediment Gradation

The theory outlined earlier is based on the assumption that the sediment is uniformly distributed with no variation in grain size and fall velocity of the suspended sediment. A rational approach to take into account the gradation of the sediment, suggested in Ref. 5, is the requirement that for a particle to go into suspension

$$\frac{w}{u_f} \leq 1 \quad \ldots\ldots (15)$$

From the distribution of particle fall velocity for a known sediment sample the critical fall velocity, w_c, can be obtained from Eq. 15. In the present, u_f has been put equal to $U_{f,max}$. Now, the sediment with a fall velocity lower than w_c is split up into three equal fractions (by volume) and the relative vertical distribution of each fraction is calculated on the basis of the mean fall velocity of each fraction.

The bed concentration of each fraction is obtained from the following two requirements:

1. The sum of the bed concentrations must be equal to that obtained by Eq. 12.
2. We consider sediment that is only moderately graded. In this case it can be assumed that the particles in suspension will keep the original composition.

The theoretical findings with graded sediment are indicated by a dotted curve in Fig. 4 and a dashed-dotted curve in Fig. 5. The deviation from the theory based on a single grain diameter is small, because the ratio $w/U_{f,max}$ is significantly below unity. However, the theory indicates a somewhat larger amount of sediment in suspension away from the bed due to the lower fall velocity of the finest fraction.

Effect of Current

The diagrams depicted in Figs. 6–8 may be helpful as a first approach to estimating the net transport in combined wave-current motion. If the current is sufficiently weak, the vertical concentration distribution is determined mainly by the wave-induced turbulence, so the transport can be estimated as the product

$$q_s \simeq \int_0^D CU\, dy \quad \ldots\ldots (16)$$

where U = the time averaged flow velocity.

In combined wave-current motion, the turbulence is not restricted to the thin oscillatory boundary layer but covers the total flow depth. For sufficiently high current velocities, this may change Figs. 6–8 considerably, especially away from the bed, where a current motion superposed upon the wave motion may increase the amount of sediment in suspension.

This increase in sediment concentration away from the bed is important, even though the concentration decreases rapidly away from the bed, because the mean current velocity increases rapidly away from the bed.

Extension of Theory to Cover Combined Wave-Current Motion.—In the following section, an extension of the model developed for pure wave motion is outlined, still based on the flow model described in Ref. 5.

In the case of a combined wave-current motion, the flow regions are split up into two (cf. Ref. 5): an inner flow region, where the flow is still treated as an oscillating boundary layer around a mean velocity profile, and an outer flow region, where the flow consists of two contributions, the wave-induced potential velocities and a steady mean current velocity. The boundary between these two regions is still considered to be time-dependent.

From this model it is possible to obtain reasonable estimates of the eddy viscosity in the combined wave current motion. In the outer region, we take the eddy viscosity to be parabolic and independent of time:

$$\epsilon_c = \kappa y U_{fc} \left(1 - \frac{y}{D}\right) \quad \ldots\ldots (17)$$

where U_{fc} = current friction velocity, which is found from the relation

$$\bar{\tau} = \rho U_{fc}^2 \quad \ldots\ldots (18)$$

where $\bar{\tau}$ = the average value of the bed shear stress in the current direction (see Ref. 6).

Inside the wave boundary layer, the eddy viscosity is taken to be time-dependent. In this region, the instantaneous velocity is given by

$$u = u_f \frac{1}{\kappa} \ln\left(\frac{y}{\frac{k}{30}}\right) \quad \ldots\ldots (19)$$

Here, we take the eddy viscosity to vary

$$\epsilon = \kappa y u_f \left[1 - \frac{y}{\delta}\left(1 - \frac{U_{fc}}{u_f}\right)\right] \quad \ldots\ldots (20)$$

so ϵ has the same parabolic shape as Eq. 11 but becomes equal to the outer eddy viscosity Eq. 17 at the top of the boundary layer.

Theoretical Results.—Fig. 9 shows an example of the distribution of the mean concentration C in combined wave-current motion. In this motion, three other parameters compared with pure wave motion are necessary in order to define the flow situation: (1) The angle γ between the

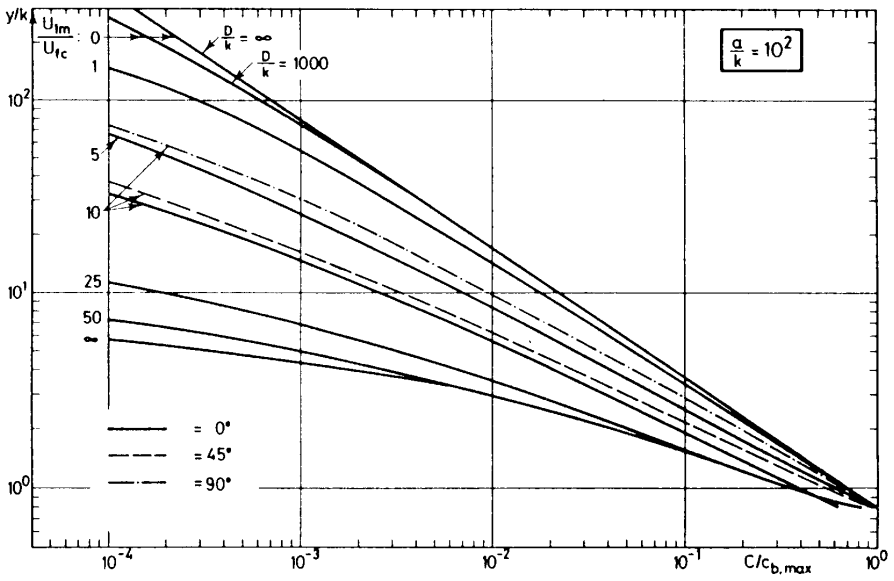

FIG. 9.—Theoretical Vertical Distribution of Average Concentration C in Combined Wave-Current Motion (a/k = 100; θ_{max} = 10; $w/U_{f,max}$ = 0.6)

current direction and the direction of wave propagation; (2) the dimensionless flow depth, D/k; and, finally, (3) the strength of the current compared with the strength of the near-bed wave-induced flow velocities. The latter can, for instance, be represented by the dimensionless quantity U_{1m}/U_{fc}. If U_{1m}/U_{fc} approaches zero, the motion approaches the pure current situation, and the distribution of the sediment will be equal to the well-known Rouse-Vanoni distribution. On the other hand, if U_{1m}/U_{fc} approaches infinity, this situation will correspond to the case of pure wave motion, so the distribution will approach the one described in the previous section.

This behavior can be seen from Fig. 9, where we have chosen to fix the parameter a/k (= 100) and vary the parameter U_{1m}/U_{fc}. The fully-drawn lines are those for $\gamma = 0$ (current direction is the same as the direction of wave propagation). It is interesting to note that in some intervals (around $U_{1m}/U_{fc} \sim 10$) the bed concentration decreases for a fixed value of θ_{max}. This is because the near-bed wave and current motions are of the same order in this interval, so when the wave-induced motion is opposite to the current motion, the bed shear stress becomes small during nearly half a wave period. If $\gamma = 90°$ this phenomenon does not occur.

For $U_{1m}/U_{fc} = 10$, Fig. 9 furthermore shows the variation in C with γ. In the three-dimensional case, more sediment will be carried in suspension if the other parameters are identical.

Comparison with Field Measurements.—While it is manageable to carry out laboratory experiments in pure wave motion with a large free stream particle amplitude (in an oscillating flume), it is difficult to make similar experiments when the waves are superposed upon a current. In the two-dimensional case, it is possible to reproduce the combined wave-current

motion by circulating the water in the oscillating flume. Measurements of suspended sediment in this flow situation have, to the writers' knowledge, not been carried out for large free stream particle amplitudes, where the bed is not covered by ripples. In the three-dimensional case, it appears difficult to make laboratory experiments.

Accordingly, the theory of suspended sediment in the combined wave-current motion is compared with field measurements from Karachi, Pakistan (10) and from the Atlantic outside the Niger Delta, Nigeria (12).

In order to compare theory and field measurements, the following procedure has been applied:

1. In the theory, the irregular waves are replaced by regular waves with height and period that equal the root-mean-square values of the irregular waves. Laboratory experiments indicate that the root-mean-square value reproduces the irregular waves best as far as the distribution of suspended sediment is concerned (14).
2. The angle between the current and the direction of wave propa-

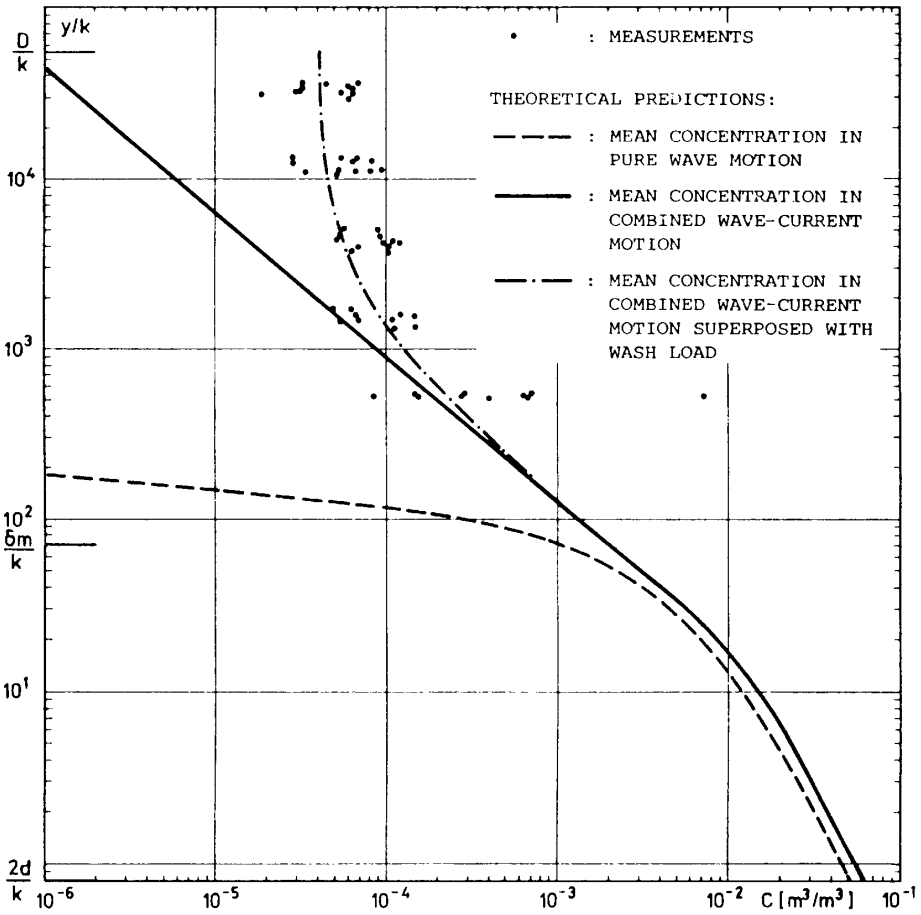

FIG. 10.—Comparison between Theory and Field Measurements, See Ref. 10 (Wave Height = 2.05 m; T = 8 s; U = 0.32 m/s; d = 0.08 mm; θ_{max} = 0.65; Estimated Amount of Wash Load: 4×10^{-5})

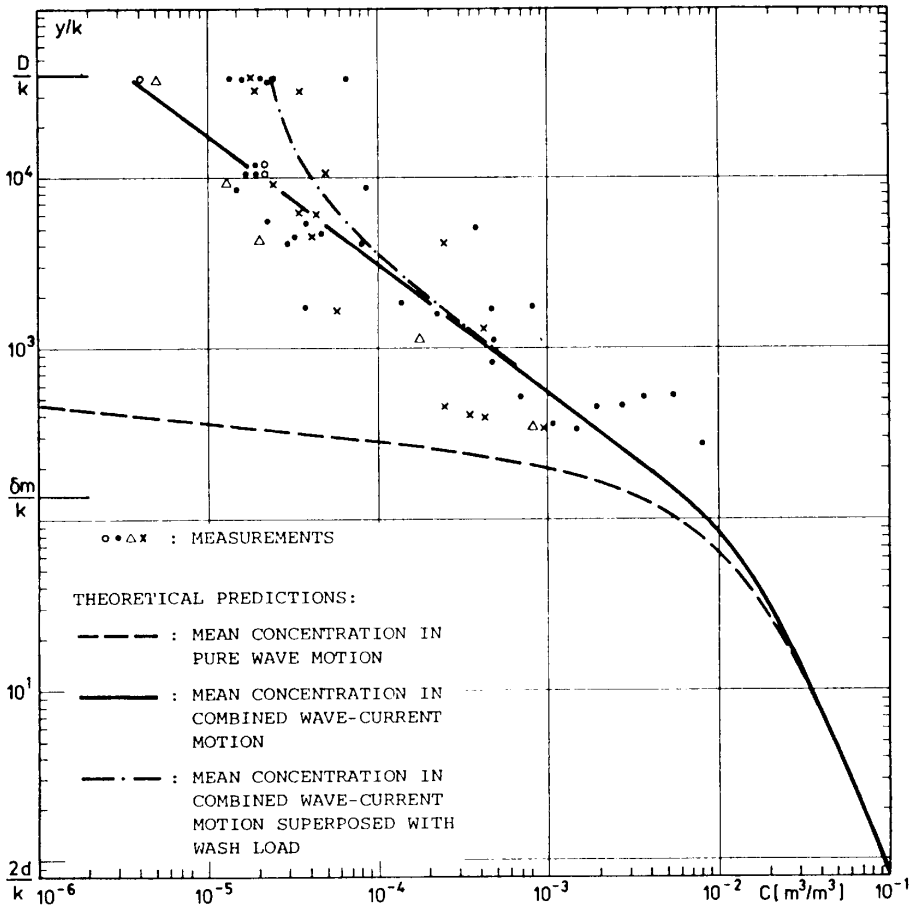

FIG. 11.—Comparison between Theory and Field Measurements, See Ref. 12 (d = 0.07 mm; Wave Height = 1.7 m; T = 12 s; U = 0.20 m/s; θ_{max} = 0.92; Wash Load: 2×10^{-5})

gation has been put equal to 90° because the field measurements are carried out not far from the coast.

3. In nature a certain amount of washload will always be present. The distribution of washload is nearly uniform over the depth and must be added to the theoretical prediction for comparison with the measurements. The content of washload is estimated to be equal to the amount of suspended sediment just below the water surface.

The fully-drawn lines in Figs. 10 and 11 are the theoretical predictions. The dashed-dotted line is the sum of the theoretical curve for suspended sand and the estimated amount of washload. Finally, the dashed curve is the theoretical prediction if the current is neglected. It is easily seen that even if this curve is superposed by a constant value of washload, it fits the measurements badly.

Conclusions

A mathematical model has been developed to describe the space and

time variations in the concentration of suspended sediment in combined wave-current motion. The model covers the general three-dimensional flow case where the current direction forms an angle with the direction of the wave propagation.

It turns out that the time variation in the concentration at a given distance from the bed is asymmetric, the rise in concentration being more rapid than the fall. This is related to the fact that the rise is caused by the increase in bounday layer thickness combined with an increase in turbulence intensity, while the fall occurs when the sediment settles with nearly the fall velocity at lower flow velocities.

Furthermore, the phase shift between maximum value of concentration and maximum value of bed shear stress increases with increasing distance from the bed.

The predictions from the theory are compared with laboratory experiments in oscillatory flow for the vertical mean concentration and for the instantaneous variation in the concentration at a certain distance from the bed.

For the pure oscillatory motion, dimensionless diagrams are included to describe the vertical mean concentration distribution.

No additional constants are introduced in the present paper.

Acknowledgments

The second writer has been supported by a grant from the Danish Technical Research Council (STVF).

Appendix I.—Numerical Solution of Diffusion Equation

The variation in c is largest close to the bed. From a numerical point of view, it will therefore be advantageous to replace the vertical coordinate y by a new variable, ζ, so the grid points in the numerical net are narrowly spaced close to the bed and more widely away from the bed. An estimate of the gradient in c close to the bed can be obtained from the steady solution. In this case, the eddy viscosity close to the bed increases linearly with increasing distance as given by

$$\epsilon = \kappa y U_f \quad \ldots\ldots (21)$$

so the steady version of the diffusion equation Eq. 1 gives

$$c = c_b \left(\frac{y}{2d}\right)^{-z} \quad \ldots\ldots (22)$$

where $$z = \frac{w}{\kappa U_f} \quad \ldots\ldots (23)$$

and is termed the Rouse number.

A suitable choice of ζ is obtained if we require

$$\frac{\partial c}{\partial \zeta} = \text{constant} \quad \ldots\ldots (24)$$

in a certain interval close to the bed.

This suggests ζ to be

$$\zeta \sim \left(\frac{-y}{2d}\right)^{-z} \quad \ldots\ldots (25)$$

If we modify Eq. 25

$$\zeta = \frac{1 - \left(\frac{y}{2d}\right)^{-z}}{1 - \left(\frac{\delta_1}{2d}\right)^{-z}} \quad \ldots\ldots (26)$$

we obtain a similar variation between y and ζ close to the bed. Furthermore, Eq. 26 takes into account the limited boundary layer thickness, which, for fine sediment, also acts as a boundary condition (cf. the correct steady solution given by Eq. 3).

In Eq. 26, we take z to be time-independent and determined by

$$z = \frac{w}{\kappa U_{f,\max}} \quad \ldots\ldots (27)$$

Now the diffusion equation can be written as

$$\frac{\partial c}{\partial(\omega t)} = \frac{a}{k} R^2(\zeta) \left[\left(\frac{\epsilon}{U_{1m}k}\right)\frac{\partial^2 c}{\partial \zeta^2} + \frac{\partial}{\partial \zeta}\left(\frac{\epsilon}{U_{1m}k}\right)\frac{\partial c}{\partial \zeta}\right]$$

$$+ \frac{a}{k} R(\zeta)\left[\frac{w}{U_{1m}} - T(\zeta)\frac{\epsilon}{U_{1m}k}\right]\frac{\partial c}{\partial \zeta} \quad \ldots\ldots (28)$$

where R and T = known functions of ζ only.

Eq. 28 is solved by applying the Crank-Nicolson implicit method in the following manner. An arbitrary vertical distribution of c at $\omega t = 0$ is chosen [e.g., $c(\zeta, 0) = 0$]. From this distribution, the distribution at a small timestep Δt later is found by application of Eq. 28. In Eq. 28, the instantaneous value of ϵ inside the wave boundary layer at time t is inserted to calculate the concentration at time $t + \Delta t$. In the case of pure waves, we put $\epsilon = 0$ outside the boundary layer $z > \delta = \delta(t)$.

Now, the calculations are carried out for so many wave periods that the boundary condition Eq. 14 is fulfilled. In the case of pure waves this occurs rather soon (normally after less than two wave periods). In the case of combined wave-current, it takes more time because the sediment is moved further away from the bed.

Appendix II.—References

1. Bagnold, R. A., "Experiments on a Gravity-Free Dispersion of Large Solid Spheres in a Newtonian Fluid Under Shear," *Proceedings of the Royal Society (London)*, Ser. A, 225, 1954, pp. 49–63.
2. Bakker, W. T., "Sand Concentration in an Oscillatory Flow," *Coastal Engineering Conference*, 1974, pp. 1129–1148.
3. Bakker, W. T., and Doorn, T., "Near-Bottom Velocities in Wave with a Current," *Coastal Engineering Conference*, 1978, pp. 1394–1413.
4. Einstein, H. A., "The Bed Load Function for Sediment Transportation in Open

Channels," U.S. Dept. Agriculture, *Technical Report, 1950, p. 1026.*
5. Engelund, F., and Fredsøe, J., "A Sediment Transport Model for Straight Alluvial Channels," *Nordic Hydrology*, 7, 1976, pp. 293–306.
6. Fredsøe, J., "The Turbulent Boundary Layer in Combined Wave Current Motion," *Journal of Hydrualic Engineering*, ASCE, Vol. 110, No. HY8, 1984, pp. 1103–1120.
7. Jonsson, I. G., *"Measurements in the Turbulent Wave Boundary Layer," IAHR,* 10th Congress 1, London, England, 1963, pp. 85–92.
8. Jonsson, I. G., and Carlsen, N. A., "Experimental and Theoretical Investigations in an Oscillatory Turbulent Boundary Layer," *Journal of Hydraulic Research*, Vol. 14, No. 1, 1976, pp. 45–60.
9. Kalkanis, G., "Transportation of Bed Material Due to Wave Action," Coastal Engineering Research Center, *Technical Memo No. 2*, 1964.
10. Kirkegaard Jensen, J., and Sørensen, T., "Measurement of Sediment Suspension in Combinations of Waves and Currents," *Coastal Engineering Conference*, Vol. 2, 1972, pp. 1097–1104.
11. Lundgren, H., "Turbulent Currents in the Presence of Waves," *Coastal Engineering Conference*, 1972, pp. 623–634.
12. Mikkelsen, L., Mortensen, P., and Sørensen, T., "Sedimentation in Dredged Navigation Channels," *Coastal Engineering Conference*, Vol. 2, 1980, pp. 1719–1734.
13. Nielsen, P., "Some Basic Concepts of Wave Sediment Transport," *Series Paper 20,* Institute of Hydrodynamics and Hydraulic Engineering (ISVA), Technical University of Denmark, 1979.
14. Rasmussen, P., and Fredsøe, J., "Measurements of Sediment Transport in Combined Waves and Current," *Progress Report No. 53*, Institute of Hydrodynamics and Hydraulic Engineering (ISVA), Technical University of Denmark, 1981, pp. 27–30.
15. Rouse, H., "Modern Conceptions of the Mechanics of Fluid Turbulence," *Transactions*, ASCE, Vol. 102, 1927, pp. 463–543.
16. Staub, C., Svendsen, I. A., and Jonsson, I. G., "Measurements of the Instantaneous Sediment Suspension in Oscillatory Flow," *Progress Report No. 58*, Institute of Hydrodynamics and Hydraulic Engineering (ISVA), Technical University of Denmark, 1983, pp. 41–49.

APPENDIX III.—NOTATION

The following symbols are used in this paper:

a = free stream particle amplitude;
C = *time-averaged concentration;*
c = instantaneous value of concentration;
c_a = concentration of suspended sediment at distance a above bed;
c_b = bed concentration, taken distance $y = 2d$ above bed;
D = flow depth;
d = *grain diameter;*
f_w = wave friction factor;
g = acceleration of gravity;
K = constant appearing in Eq. 5;
k = bed roughness;
q = *volumetric sediment transport rate;*
s = relative density of sediment;
T = wave period;
t = time;
U = time-averaged flow velocity;
U_f = *mean value of friction velocity;*

U_{f1} = mean value of friction velocity according to mean flow velocity V_1;
U_{fc} = current friction velocity;
$U_{f,\max}$ = maximum friction velocity;
U_{1m} = maximum velocity in wave motion just outside wave boundary layer;
u = instantaneous flow velocity;
u_f = instantaneous value of friction velocity;
u_0 = instantaneous flow velocity outside boundary layer;
V_1 = mean flow velocity over vertical;
w = fall velocity of sediment grains in suspension;
y = distance from bed;
γ = angle between current and waves;
δ = instantaneous wave boundary layer thickness;
δ_1 = mean wave boundary layer thickness;
ϵ = instantaneous eddy;
ϵ_s = turbulent exchange factor for sediment;
ϵ_w = average eddy viscosity in pure wave motion;
$\bar{\epsilon}$ = time-averged eddy viscosity;
ζ = dimensionless vertical coordinate;
θ = dimensionless bed shear stress;
$\theta_{\max}$ = maximum dimensionless bed shear stress;
κ = von Kármán's constant;
ρ = fluid density;
τ = bed shear stress;
$\bar{\tau}$ = mean bed shear stress;
ϕ = phase between maximum bed shear stress and maximum velocity; and
ω = angular frequency.